Incorporation of Elastic Transformations in List-Mode Based Reconstruction for Respiratory Motion Correction in PET

F. Lamare, *Member, IEEE,* M.J. Ledesma Carbayo, *Member, IEEE,* G. Kontaxakis, *Member, IEEE,*
A. Santos, *Senior Member, IEEE,* A. Turzo, Y. Bizais, C. Cheze Le Rest, and D. Visvikis, *Member, IEEE*

Abstract— Respiratory motion in emission tomography leads to reduced image quality. Proposed correction methodology has been concentrating on the use of respiratory synchronised acquisitions leading to gated frames. Such frames however are of low signal to noise ratio as a result of containing reduced statistics. Therefore a method accounting for respiratory motion effects without affecting the statistical quality of the reconstructed images is necessary. In this work we describe the implementation of an elastic transformation within a list-mode based reconstruction for the correction of respiratory motion over the thorax. The developed algorithm was evaluated using datasets of the NCAT phantom generated at different points throughout the respiratory cycle. List mode data based PET simulated frames were subsequently produced by combining the NCAT datasets with a Monte Carlo simulation. Transformation parameters accounting for respiratory motion were estimated according to an elastic registration of the NCAT dynamic CT images and were subsequently applied during the image reconstruction of the original emission list mode data. The One-pass list mode EM (OPL-EM) algorithm was modified to integrate the elastic transformation. The corrected images were compared with those produced using an affine transformation of list mode data prior to reconstruction, as well as with uncorrected respiratory motion average images. Results demonstrate that although both correction techniques considered lead to significant improvements in accounting for respiratory motion artefacts in the lungs and heart, the elastic transformation based correction leads to a more uniform improvement across the lung field for different lesion sizes.

Index Terms— PET, respiratory motion correction, list-mode, image recontruction, elastic registration.

I. Introduction

RESPIRATORY motion artefacts lead to reduced image quality and quantitation in thoracic emission tomography imaging. In addition, the advent of combined imaging devices such as PET/CT and SPECT/CT, have placed increased emphasis in respiratory motion related effects, further highlighting the need for respiratory motion correction.

Currently proposed methodology for reducing the effects of respiratory motion have been based on the development of

respiration gated acquisitions leading to a number of frames corresponding to different parts of the respiratory cycle. However, the result of such multi-frame acquisitions lead to gated images suffering from poor signal to noise ratio since each of the frames contain only part of the counts available throughout the acquisition of a respiration average PET study [1]. Therefore the need exists for the development of methodology that corrects for respiratory motion effects between individual gated frames in order to allow the use of the data available throughout a respiratory cycle. In an attempt to make use of all data available throughout a respiratory gated acquisition, we have recently evaluated a method using an affine transformation of list-mode data prior to reconstruction. The implementation of a transformation methodology on raw data should lead to improved image quality in terms of contrast and signal to noise ratio in comparison to an image based transformation. This method leads to significant improvement in terms of recovered activity concentration and position of pulmonary lesions [2]. However, this technique is based on the use of a unique set of transformation parameters for the entire field of view (FOV). Consequently, the accuracy of the achieved correction depends on lesion location in the lung field and organs below the diaphragm are equally not well corrected [2]. On the other hand, the use of an elastic model based transformation may more accurately account for respiratory movements throughout the imaging FOV.

Although the application of an affine transformation in the raw data domain is feasible considering individual lines of response, a similar approach for elastic transformation poses obvious challenges. The objectives of the presented work have been the implementation and validation of a motion correction technique based on the incorporation of an elastic transformation as part of the reconstruction algorithm for list mode data.

II. Materials and Methods

A Monte-Carlo simulator combined with the NCAT phantom was used to produce PET respiratory gated acquisitions. In the clinical case, the transformation may be obtained through the use of dynamic (respiratory gated) CT datasets [3]. For the simulated frames the amplitude of the different organ motion as a result of respiration was derived by performing elastic or affine registration on the original NCAT attenuation images.

Details on the affine registration algorithm used have been presented in [2].

A. NCAT phantom

A digital NURBS based 4D cardiac-torso phantom (NCAT) was used [4]. A number of different size (7, 11, 15, 21mm) lesions were included at different locations throughout the lungs. Eight NCAT emission images were produced, corresponding to 0.625s considering a normal respiratory cycle of 5s. The generated NCAT attenuation / CT images without any blurring effects (resolution, image statistics effects, etc) were used in combination with the elastic registration to define the transformation fields to be used during the reconstruction of the simulated list mode emission data.

The first frame represents full exhalation, while the maximum magnitude of respiratory motion (full inspiration) is occurring between the 4^{rth} and 5th frames. Deformation matrices were derived between all individual frames and that corresponding to full exhalation (i.e. frame 1).

B. Elastic transformation fields

Elastic registration of the NCAT CT frames was performed using a spatio-temporal algorithm for motion reconstruction from a series of images. This method uses a semi-local spatio-temporal parametric model for the deformation using B-splines and reformulates the registration task as a global optimization problem [5].

C. Simulation system

The model of a clinical PET system [6] developed with GATE (Geant4 Application for Tomographic Emission) was combined with the NCAT phantom in order to obtain dynamic emission frames acquired throughout a respiratory cycle. The attenuation images of the NCAT phantom were also integrated in order to simulate the effects of attenuation. Finally, the data simulated for each individual frame was saved in list mode format.

D. Image reconstruction on list-mode data

The One-pass list mode EM (OPL-EM) algorithm [7] was implemented for the reconstruction of the transformed LORs:

$$n_j^{k+1} = \frac{n_j^k}{s_j} \sum_{i \in T^k} a_{ij} \frac{1}{q_i^k} \qquad for \; k = 1, ..., K \qquad (1)$$

where $q_i^k = \sum_{j=1}^{J} a_{ij} n_j^k$ is the expected count in LOR i, n_j is the intensity of voxel j, J is the total number of voxels, s_j is the voxel j of the sensitivity image including the normalisation and attenuation corrections, and K is the number of time-subsets. k is both the iteration number and the subset used in that iteration. T^k is the set of list mode events in the kth subset. The accelerated version of the Siddon ray tracing [8] was used to implement the forward projection [9, 10].

(a). (b).

(c). (d).
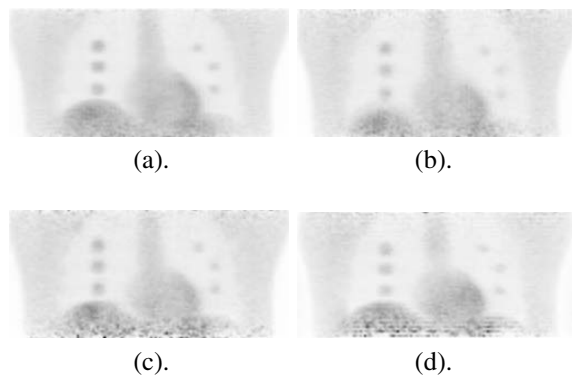
Fig. 1. Comparison of the Frame1 (a), non-corrected (b), LORs-Affine (c) and Elastic (d) images. Visual differences can be clearly seen at the level of the liver.

Three different reconstructions were performed:

- The 8 temporal frames were summed without any transformation and reconstructed (Non-corrected image).
- Each of the list-mode files corresponding to the last 7 frames were corrected using the affine registration parameters. They were subsequently summed together and reconstructed (LORs-Affine image) [2].
- The elastic transformation fields were included during the reconstruction of the corresponding list-mode datasets (Elastic image). The implementation of the elastic transformation in the reconstruction process is described in section 2E.

Images of $128 \times 128 \times 60$ with a voxel size of $3.125 \times 3.125 \times 3.125 \text{mm}^3$ were obtained for each of the reconstructed temporal NCAT frames. For a list mode dataset of 5.4million detected coincidences, an iteration of the OPL-EM algorithm was <10min for an image of the above dimensions (Pentium IV, 2.8Ghz). A total of 7 iterations were found to be optimum for the reconstruction of the NCAT images.

Normalisation and attenuation corrections were performed through a forward projection and backprojection of the NCAT attenuation images in order to produce a sensitivity image S including the normalisation and attenuation corrections for each of the individual simulated frames.

Each voxel s_j of the sensitivity image S is computed as follows:

$$s_j = \frac{1}{T} \int_T \sum_{i \in I} a_{ij} A_i \; \text{with} \; A_i = exp(-\sum_{j=1}^{J} a_{ij} \mu_j)$$

A_i is the attenuation correction factor of the LOR i. I is the total number of detectable LORs, J is the total number of voxels and μ_j is the linear attenuation coefficient at the energy of 511keV (μ_j is the intensity of the voxel j in the NCAT attenuation image). T is the acquisition time.
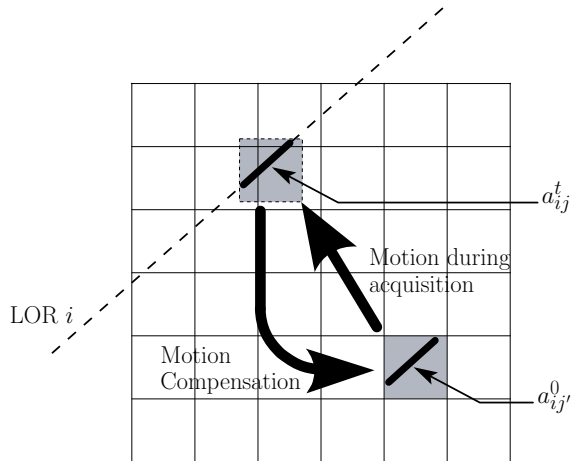
Fig. 2. Graphical representation of the incorporation of the elastic motion compensation during recontruction.

E. Implementation of the elastic transformation on the list mode data

The discrete motion transformation field ζ_t contains 3D vectors describing individual voxel motion parameters, such that a voxel j' at time $t_0 = 0$ has been moved to the location $j = \zeta_t(j')$ at acquisition time t (due to object motion). These transformation fields are provided by the elastic registration. It is worth noting that the voxel j' at time $t_0 = 0$ (reference image = NCAT frame 1) corresponds to an actual grid voxel, whereas the voxel $j = \zeta_t(j')$ can overlap several voxels of the grid (see figure 2).

$$\zeta_t : \left\{ \begin{array}{c} \text{reference} \\ \text{image } (t_0) \end{array} \right\} \quad \rightarrow \quad \left\{ \begin{array}{c} \text{image at} \\ \text{time } t \end{array} \right\}$$
$$\text{voxel } j' \quad \rightarrow \quad \text{voxel } j = \zeta_t(j')$$

Assume a_{ij} is the geometric probability of detecting at LOR i an event generated in voxel j, in the initial position before any motion. a_{ij} corresponds to the overlap between a voxel j and a LOR i. It has to be noted that, the overlap between a voxel j and an LOR i at time t is equivalent to the overlap with the transformed voxel j' had the object not moved (reference acquisition time = 0) (see figure 2):

$$a_{ij}^t \delta_j \equiv a_{ij'}^0 \text{ ,where } j = \zeta_t(j') \quad (2)$$

where i is the index of the detected LOR, j is the index of the voxel at acquisition time t, and j' those of the corresponding motion corrected voxel at time $t_0 = 0$. The function δ_j is defined by:
$\delta_j = \left\{ \begin{array}{l} 1, \text{ if the voxel } j \text{ at time } t \text{ is inside the grid} \\ 0, \text{ otherwise} \end{array} \right.$

The reconstructed image will represent the activity concentration at time $t_0 = 0$, had the object not moved. During the reconstruction process, all the coefficients $a_{ij}^t \delta_j$ will be computed, but the result will be applied to the voxel j'.

The sensitivity image S used to correct for attenuation and normalisation has to equally take into account the motion correction of the voxel location. Therefore the coefficients s_j of the sensitivity image S are now defined as:

$$s_{j'} = \frac{1}{T} \int_T \sum_{i \in I} a_{ij'} A_i \text{ , with } A_i = exp(-\sum_{j'=1}^{J} a_{ij'} \mu_{j'})$$

A_i is the attenuation correction factor of the transformed LOR i. I is total number of detectable LORs, J is the total number of voxels and $\mu_{j'}$ is the linear attenuation coefficient at the energy of 511keV in the initial position ($\mu_{j'}$ is the intensity of the voxel j' in the NCAT attenuation image). T is the acquisition time.

F. Image analysis

The motion corrected images (LORs-Affine and Elastic) were compared to the first temporal frame (reference image). The total number of coincidences were kept the same for all images in order to distinguish the effects purely associated with motion, rather than including those arising from differences in statistical quality between the single temporal frame (including only part of the data) and the corrected frames (including all of the available data). In order to better quantify motion compensation, we have also compared the two corrected images (LORs-Affine and Elastic) with the respiratory average image.

The contrast and FWHM improvements are computed as follows:

$$\% \, improvement = \frac{|original \, error - remaining \, error|}{|original \, error|}$$

$\text{with} \left\{ \begin{array}{l} original \, error = |Non\text{-}corrected - Frame1| \\ remaining \, error = |Corrected - Frame1| \end{array} \right.$,

where $Corrected$ can be the $Elastic$ or the $LORs - Affine$ image.

To assess the improvement in terms of contrast in the reconstructed images, regions of interest (ROI) were placed in each of the lung lesions and in the background lung. The slice with the maximum count density over the lesion was identified for the ROI analysis. Average count densities were subsequently derived for each lesion.

On the other hand to quantify the position and "spreading" improvement as a result of the motion compensation, line profiles were drawn in the x, y and z directions for each lesion. Each of the lung lesion profiles was subsequently fitted with a gaussian in order to derive the position and FWHM in all three dimensions.

III. RESULTS

Figure 3 contains the % contrast improvement results as a function of lesion size location for the two respiratory motion corrected images (LORs-Affine and Elastic). A qualitative assessment in terms of lesion and liver location with and without motion correction is shown using a profile across the reconstructed image as illustrated in figure 4. On the other hand, figures 5 and 6 contain quantitative results on position and FWHM improvements respectively.
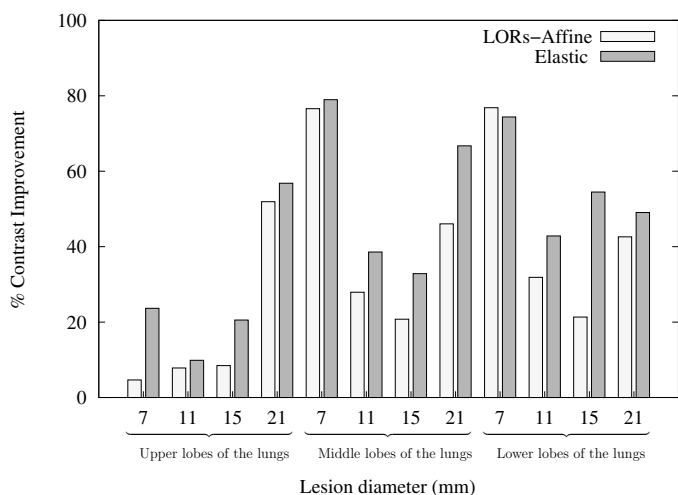
Fig. 3. Contrast improvement due to the two respiratory motion correction techniques.
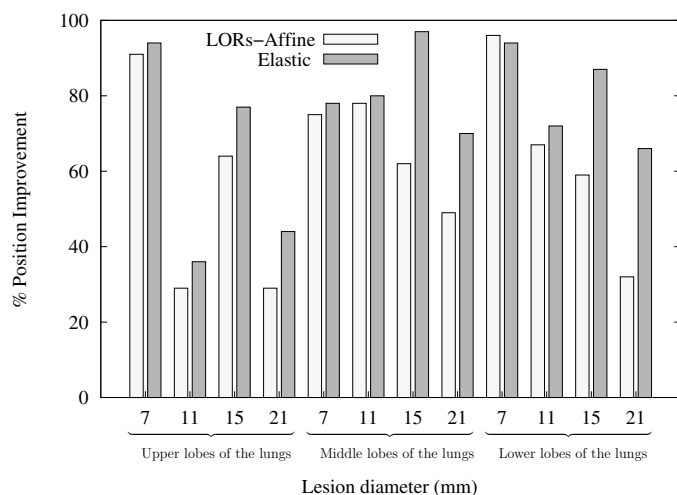
Fig. 5. Position improvement along the Z axis due to the two respiratory motion correction techniques.
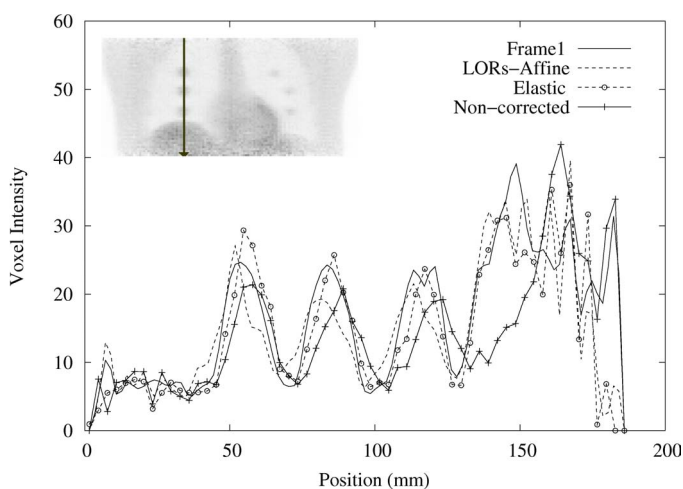
Fig. 4. Profile of the lung lesions and the liver along the Z axis.
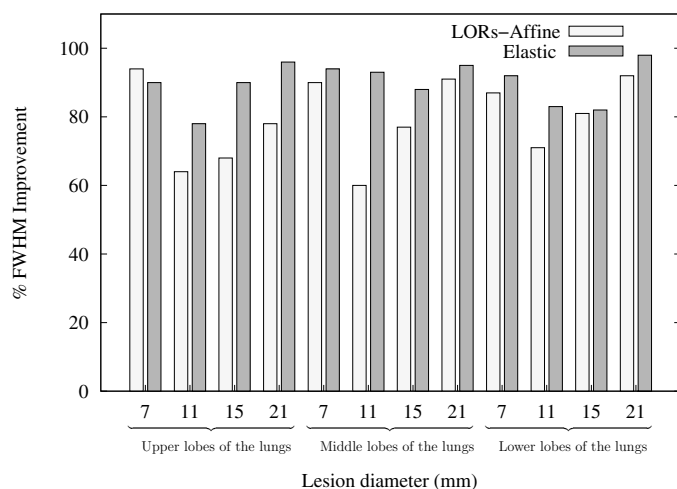
Fig. 6. FWHM improvement along the Z axis due to the two respiratory motion correction techniques.

IV. DISCUSSION

The solutions that have been proposed to date for taking into account the effects of respiratory motion concentrate on the acquisition of respiration synchronised PET and CT datasets. Irrespective of the gating methodology implemented the emission data acquired in each of the temporal gated frames is reasonably free of respiration produced inaccuracies. However, the resulting individual frame images are of reduced resolution as well as overall quality as they contain only a fraction of the counts available throughout a PET acquisition. Therefore the need exists for the development of correction methodologies, making use of the gated datasets, in order to obtain respiration free PET images using all available data throughout a standard respiration average PET acquisition. This approach will also remove the need currently existing in terms of significantly increasing the time (over a factor of 3) of gated PET acquisitions in order to compensate for the presence of reduced statistics in the final reconstructed images. Very limited

work is currently available in this domain. Our objective in this study has been to assess the improvement that can be obtained in terms of lesion contrast and location as a result of correcting gated raw list mode datasets for the presence of respiratory motion through the application of an elastic transformation during the reconstruction process.

Our study was based on the use of the NCAT phantom with the introduction of variable size and location lesions in the lung field and in the liver. Elastic transformation fields were derived by using the high resolution NCAT phantom based CT attenuation maps. The OPL-EM algorithm was adapted to integrate the elastic transformation during the reconstruction process. Dedicated attenuation and normalisation corrections were also developed to take into account the applied elastic transformation. The results obtained at that stage of our investigation allowed us to predict a considerable improvement in the lung and cardiac fields through the application of an elastic

transformation.

The elastic method was also compared with an affine transformation based respiratory motion correction where the transformation of list mode data takes place prior to the reconstruction. As figure 3 demonstrates an improvement of ∼10-80% in terms of contrast can be obtained on lung lesions in the corrected images depending on lesion location and size. A larger improvement was generally observed for smaller lesions, although the 7mm lesion results suffer from significant partial volume effects. In addition, the corrected images using the elastic transformation lead to improvements in terms of contrast of up to 30% in comparison to the affine transformation based correction.

As far as improvement in the recovered lesion location a larger correction effect was observed along the Z axis, where respiratory motion effects are more significant. Using the Z direction profiles from figure 4, one can appreciate that the displacement of the lesions and the liver has been well corrected by comparison to the NCAT gated frame 1 and the uncorrected respiration average image. Along the Z axis, the average remaining error for all the lesion sizes on the three lung lobes is about 2.7mm (with an average improvement of 9.46mm in comparison to non-corrected images). Similar to the contrast results, the elastic transformation method leads to improved lesion location by up to 30% in the case of lesions >1cm. In the case of smaller lesions the accuracy in the determined lesion positioning is compromised by the relatively large reconstructed pixel size. As a result no significant improvement is seen using the elastic transformation for lesions < 1cm irrespective of lesion location.

Concerning the FWHM of the lesion profiles along the Z axis, the maximum improvement is up to 95% for the three lobes of the lungs. For the three parts of the lung considered, the maximum improvement is obtained for the bigger lesions, considering that on this parameter investigation we are once more limited by the relative size of the smaller lesions in comparison to our reconstructed pixel size. However, figure 6 clearly illustrates a more uniform magnitude of improvement in the FWHM of the lesions in the corrected images using the elastic transformation based solution throughout the lung fields.

V. CONCLUSION

A list-mode data based respiratory motion correction using elastic transformation during image reconstruction has been implemented and its performance evaluated. The developed algorithm includes the implementation of a normalisation correction taking into consideration the applied transformation.

A comparison of the reconstructed images with and without correction revealed significant respiratory motion compensation in the lung lesions. In comparison to the use of an affine model, the elastic transformation based solution leads to a more uniform improvement across the lung field for the different lesion sizes considered.

REFERENCES

[1] L. Boucher, S. Rodrigue, R. Lecomte *et al*, *Respiratory gating for 3D PET of the thorax: feasibility and initial results*, J Nucl Med, 45, 214-219, 2004.

[2] F. Lamare, T. Cresson, S. Savean, C. Cheze Le Rest, A. Turzo, Y. Bizais, D. Visvikis, *Affine Transformation of List-mode Data for respiratory motion correction in PET* IEEE MI conference records 2004.

[3] S.A Nehmeh, Y. Erdi, T. Pan *et al*, *Quantification of respiratory motion during 4D PET/CT acquisition* Med Phys 31(6), 1333-1338, 2004

[4] W.P. Segars, D.S. Lalush, B.M.W Tsui, *Modelling respiratory mechanics in the MCAT and spline-based MCAT phantoms*, IEEE Trans Nuc Sc, 48(1), 89-97, 2001.

[5] M.J Ledesma-Carbayo, J. Kybic, M. Desco, A. Santos, M. Suhling, P. Hunziker, M. Unser, *Cardiac motion analysis from ultrasound sequences using non-rigid registration* IEEE Trans Med Imag, 1113-1126, 2005

[6] F. Lamare, A. Turzo, Y. Bizais,D. Visvikis *Simulation of the Allegro PET system using GATE*, SPIE MI Conference records, 2004.

[7] A.J. Reader, S. Ally, F. Manavaki, R.J. Walledge, A.P. Jeavons *et al* *One-pass list-mode EM algorithm for high-resolution 3D PET image reconstruction into large array*, IEEE Trans Nucl Sci, 49(3), 693-699, 2002.

[8] G. Han, Z. Liang, J. You *A fast Raytracing Technique for TCT and ECT Studies*, IEEE MI Conference records, 1999.

[9] R.L. Siddon *Fast calculation of the exact radiological path for a three-dimensional CT array*, Med. Phys., 12, 252-255, 1986.

[10] H. Zhao, A.J. Reader *Fast Projection algorithm for voxel arrays with object dependent boundaries*, IEEE MI Conference records, 2002.